HIGH-RESOLUTION SEISMIC IMPEDANCE INVERSION USING IMPROVED CEEMD WITH ADAPTIVE NOISE

ABOLFAZL KHAN MOHAMMADI, REZA MOHEBIAN and
ALI MORADZADEH

School of Mining Engineering, College of Engineering, University of Tehran, Tehran, Iran. Mohebian@ut.ac.ir

(Received February 21, 2021; revised version accepted August 2, 2021)

ABSTRACT

Khan Mohammadi, A., Mohebian, R. and Moradzadeh, A, 2021. High-resolution seismic impedance inversion using improved CEEMD with adaptive noise. *Journal of Seismic Exploration*, 30: 481-504.

Seismic impedance inversion is an inevitable step in reservoir characterization required in both exploration and field works. It provides layer-based acoustic impedance property of rocks by imaging subsurface through the integration of data derived from seismic and well logging investigations. Recent studies providing subsurface rocks' properties have highlighted the need to resolve seismic data's nature, which is the limited frequency bandwidth. Although a significant amount of work has been done in the previous years by geophysicists, this problem continues. In this study, by implementing a powerful and robust time-frequency signal processing method, namely improved complementary ensemble empirical mode decomposition with adaptive noise (ICEEMDAN), we propose a seismic inversion algorithm in order to overcome the mentioned problem. In other words, we propose an algorithm that improves the seismic impedance inversion in order to obtain subsurface images with higher resolution than other common impedance inversion methods. For a dataset, the proposed method resulted in a 98.44(%) correlation coefficient with 164.82 RMS error between the original log and inverted log while the commercial Band-limited, hard and soft constrained Model-based inversion methods resulted in a 91.29(%), 91.12(%) and 93.05(%) with 345.33, 322.39 and 295.48 RMS errors, respectively. Results demonstrate the resolution enhancement in impedance inversion by our proposed method in comparison to previous approaches.

KEY WORDS: seismic inversion, acoustic impedance, empirical mode decomposition, improved CEEMD, F3 block.

0963-0651/21/$5.00

INTRODUCTION

Seismic inversion provides subsurface physical models with rocks' and fluids' characteristics. This tool frequently employs seismic data to integrate with information derived from well log to calculate the physical properties of subsurface layers (Pendrel, 2006). The physical parameters are the P-impedance, S-impedance, velocity, density, and porosity. Interpreting seismic data solely is a predicament, so inversion-based attributes are utilized to enhance the interpretation (Chen and Sidney, 1997). The seismic impedance inversion methods became prevalent when extraction of phase spectra for wavelets as well as their amplitude through computation became available (Lindseth, 1979). Seismic inversion aims to engender high-resolution subsurface images to enhance the interpretation of seismic data and essentially reduce the drilling risk and cost (Pendrel, 2006). Seismic acoustic impedance inversion has several restraints:

- A conventional seismic frequency band is often constrained to a usable bandwidth of 8-80 Hz in marine environments. On the other hand, in broadband seismic acquisition systems, the usable frequency bandwidth ranges from 2.5 Hz up to 200 Hz or more for shallow targets. But, in most cases, below 8 Hz, and over 80 Hz frequencies are barely available in marine cases (Amundsen and Landrø, 2013).
- Some obstacles are preventing seismic inversion from producing its intended goal. These obstacles are multiples, reflections, transformation losses, acquisition patterns, and frequency-dependent retention due to acquiring appropriate seismic gathers for interpretations and inversion (Carrazzone et al., 1996).
- Non-uniqueness of the seismic inversion results cause numerous conceivable geologic models consistent with observations (Latimer et al., 2000).

To alleviate these unreliable factors in the inversion procedure, additional information is required. These can be derived from well logging that includes the low and high frequency components within a range of 0 to approximately 200 Hz and even more (depending on the sampling frequency of the well log). These crucial frequency components are usually employed to restrict the divergency in the initial model estimation procedure (Ferguson and Margrave, 1996; Russell, 1988). The final inversion results in a subsurface model depending on the seismic data quality, while its initial model or its low frequency information comes from the data derived from well logging techniques and the ill pose problem caused by the lack of high and low frequency components in the data is solved (Gholami, 2016; Liu et al., 2015; Lloyd, 2013). However, the inversion algorithm itself is another factor that plays an important role in affecting the resolution of the intended output (Maurya and Singh, 2019; Maurya et al., 2020; Schuster, 2017).

This research aims to consider a robust method in order to acquire high-resolution subsurface images by using the most available frequency components in the data, and reducing the frequency losses in the seismic impedance inversion procedure. Stochastic seismic inversion has been proposed to obtain subsurface information, especially in the case of the thin layer investigations (Grant et al., 2017; Li et al., 2019; Zhang et al., 2012). Further, (Ray and Chopra, 2016) proposed multi-attribute regression analysis with cross validation. Multiple multi-attribute impedance inversion methods have been proposed (Alvarez et al., 2015; Fnegqi et al., 2014; Haris et al., 2017; Zahmatkesh et al., 2018) for seismic impedance inversion to acquire high resolution and more robust acoustic impedance models. Also, (Zhou et al., 2019) proposed a multi-trace basis-pursuit seismic inversion method to improve the outcome resolution for seismic investigations. Inversion and imaging have been well studied using computer science, and geophysics and multiple powerful algorithms have been proposed to obtain high-resolution images for interpretation (Maurya et al., 2020; Schuster, 2017; Wang, 2016). Some recent scholars have improved seismic inversion methods by implementing newer autonomous techniques (Das et al., 2018; Kushwaha et al., 2020; Yang and Ma, 2019).

In this paper, we use a powerful and recently developed time-frequency signal processing method based on empirical mode decomposition (EMD) that decomposes any time series into its intrinsic mode functions (IMF). Each IMF represents different frequency elements of the initial signal. We use the improved complementary ensemble EMD with adaptive noise (ICEEMDAN) time-frequency analysis (TFA) method (Colominas et al., 2014; Han and van der Baan, 2013; Shangyue et al., 2015). The first IMF contains the highest frequencies available in the initial signal, and the last IMF or the residual contains the lowest frequency components in the mother signal while it gives the linear trend of it (Jicheng et al., 2020; Xue et al., 2019; Zhang et al., 2018; Zhang and Li, 2020). By implementing the ICEEMDAN in the seismic impedance inversion, we separate the frequency components of the well log signal precisely and extract the necessary components for the inversion procedure.

In other words, our seismic inversion algorithm uses ICEEMDAN in order to compute the acoustic impedance with more accuracy. Our method results in a higher resolution impedance model in comparison to the commercial band-limited and model-based inversion approaches. Finally, we compared our results with other commercial impedance inversion methods to illustrate the resulting accuracy, and multiple cross plots are provided in order to demonstrate the advantages of our approach.

THEORY AND METHODOLOGY

As our proposed algorithm uses the improved CEEMDAN, a brief review of its concepts is given here.

EMD

EMD decomposes the initial signal into several signals called IMFs or intrinsic mode functions and a residual signal in an iterative procedure. Each of them describes the oscillations inside the primary signal. With a simple summation, they can rebuild the initial signal regardless of a mixing problem. These IMFs must have two following characteristics:

- The number of extrema and zero crossings have to either be equal or differ by one (maximum) in the entry signal to the decomposition procedure.
- At any random point in the mother signal (initial signal), the mean value of the envelope constrained to the local maxima and minima must be zero.

These conditions are vital to assure that every IMF has a localized frequency content by avoiding frequency spreading due to asymmetric waveforms (Bekara and van der Baan, 2009; Han and van der Baan, 2011; Huang and Wu, 2008).

EMD is a fully data-driven signal decomposition tool. It decomposes the entry signal into a series of functions with fast and slow oscillations or high and low frequencies, respectively. These IMFs are computed recursively of which the first of them is the most oscillatory or the highest frequency contained component. The algorithm proposes a cubic spline interpolation method to calculate the local maxima to construct the upper bound once the maxima of the initial signal have been defined. The same process is used for local minimum amplitudes to acquire the lower bound. These bounds are called envelopes. In the next step, the algorithm proposes subtracting the mean of the upper and lower envelopes to extract the first IMF inside the initial signal. This interpolation is proceeded on the leftover portion and called the *Sifting* procedure, which concludes when the average envelope is roughly zero everywhere. The resulting signal is denoted as IMF_1. This function is also known as the first oscillatory component of the original signal which is derived by the EMD method (Han and van der Baan, 2013; Huang et al., 1998; Huang and Wu, 2008). The algorithm for EMD is written below, which is necessary for ICEEMDAN.

The first IMF is subtracted from the mother signal in order to consider the residual signal as a new input, and the same *Sifting* procedure must be applied to it to acquire the subsequent IMF. This process is stopped once the final IMF has a roughly zero amplitude or becomes monotonic, which only contains the signal's linear trend (Han and van der Baan, 2011, 2013; Huang and Wu, 2008; Mhamdi et al., 2010).

The frequency mixing problem which is also known as the mode mixing problem, is an obstacle to decompose the initial signal to diverse signals with independent frequency content. Mode mixing is characterized as a single IMF including signals with broadly dissimilar scales or a signal of a comparable scale residing completely various IMF components. In other words, a single IMF contains other IMF's components, which is the definition of the mode mixing problem (Huang and Wu, 2008).

In order to solve the mode mixing problem, several approaches have been established. One of them is ensemble empirical mode decomposition (EEMD). According to the filter bank structure of the EMD and to address the mentioned issue, a noise-assisted method has been proposed, which stabilizes the *Sifting* process and its performance by adding Gaussian noise to the original signal (Flandrin et al., 2004; Wu and Huang, 2009). To implement this method, a series of steps have been defined in Fig. 1.

Algorithm 1 Empirical Mode Decomposition algorithm

Inputs:
Initial signal as x
Maximum iteration as MaxIt

Outputs:
IMFs
Residual

```
function EMD(x)
    IMF = {}
    k = 1, j = 1                ▷ j = number of IMFs        ▷ k = iteration number
    residue = x
    l1 = residue
    while amplitude of residue ≠ 0 do
        while number of extremas of lk ≥ 2 || k ≠ MaxIt do
            EnvAverage(lk)                                  ▷ envelopes average
            calculate the average of local extermas of lk via cubic spline interpolation
            return Z(lk)
            lk = lk − Z(lk)
            k = k + 1
        end while
        IMFj = lk
        residue = residue - IMFj
        j = j + 1
    end while
    Residual = x - IMF(1, ⋯, j)
    return IMFs, Residual
end function
Close all processes
```

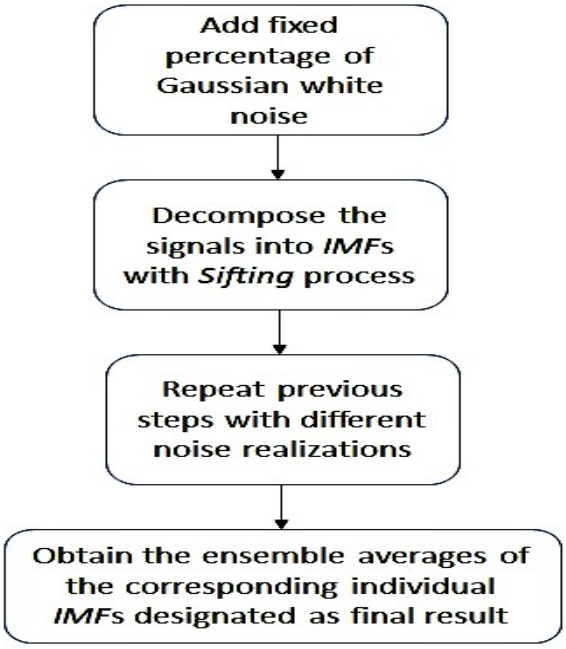

Fig. 1. Ensemble empirical mode decomposition workflow.

The introduced Gaussian white noise sequences in the algorithm are zero mean with a constant flat-frequency spectrum. Their participation in this way counteracts and does not produce the signal components that are not existed in the mother signal. Subsequently, the ensemble-averaged EMD components preserve their inherent dyadic characteristics and eliminate the chance of the frequency mixing efficiently. Consequently, EEMD compensates for EMD's weakness and improves its performance. However, a question should be answered: does this method decompose the original signal properly? In other words, does the summation of all extracted IMFs will reconstruct the initial signal precisely? Due to the algorithm's architecture, each noise-assisted EMD application can extract a various number of IMFs. The result of the summation of extracted IMFs is not the original signal precisely, while the error of rebuilding increases, which depends on the number of implicated noise realizations with an increment in computation time.

CEEMDAN

Complete ensemble EMD using adaptive noise (CEEMDAN) is also a noise-assisted method which process contains three steps (Han and van der Baan, 2011, 2013; Torres et al., 2011; Xue et al., 2016, 2019; Yeh et al., 2010; Zhang et al., 2018):

- The primary step is to include a fixed-rate Gaussian white noise onto the original signal. Then it will calculate IMF_1 from the data blended with noise. According to eq. (1), after repeating the decomposition cycle *i* times with various noise realizations, the original signal's first mode (IMF_1) will be obtained.

$$IMF_1 = \frac{1}{I}\sum_{i=1}^{I} E_1[x + \epsilon w_i]. \tag{1}$$

where IMF_1 is the first EMD component of the initial signal x, W_i is zero means Gaussian white noise with unite variance, ε is a fixed coefficient, E [ ] extracts the i-th IMF component, and I is the number of realizations in eq. (1).

- In the next step, the first signal residue r_1 is calculated by eq. (2),

$$r_1 = x - IMF_1. \tag{2}$$

- In the last step, decompose realizations $r_1 + \varepsilon\, E_1[w_i]$, $i = 1,2,...,I$, until they reach their first IMF conditions and calculate the ensemble average as the second IMF_2 according to eq. (3)

$$IMF_2 = \frac{1}{I}\sum_{i=1}^{I} E_1[r_1 + \epsilon E_1 w_i]. \tag{3}$$

For $j = 2,3,...,J$, same as all previous steps for first and second IMFs, the first component of $k + 1$'s IMF will be calculated with eq. (5) in an iterative manner. Before that, the J-th residue must be calculated with eq.(4), according to $r_j + \varepsilon\, E_j[w_i]$, $i = 1,2,...,I$.

$$r_j = r_{j-1} - IMF_j, \tag{4}$$

$$IMF_{j+1} = \frac{1}{I}\sum_{i=1}^{I} E_1\left[r_j + \epsilon E_j w_i\right]. \tag{5}$$

The *Sifting* process iterates till the last residue does not have more than two extrema, producing eq. (7) considering eq. (6)

$$R = x - \sum_{j=1}^{J} IMF_j, \tag{6}$$

$$x = \sum_{j=1}^{J} IMF_j + R. \tag{7}$$

in which R is the final IMF (residual) and J is the total number of the intrinsic mode functions. Eq. (7) is the factor that makes the CEEMDAN a complete decomposition (Han and van der Baan, 2013; Torres et al., 2011; Xue et al., 2016; Yeh et al., 2010; Zhang et al., 2018). CEEMDAN has two advantages analogous to EMD and EEMD:

- Solves the difficult to overcome mode mixing problem properly.
- Reduces the error derived from reconstructing the original signal from extracted IMFs to almost zero due to its exactness.

The previous studies showed that the CEEMDAN method has advantages over both EEMD and EMD. However, two technical problems that still go on with this method, are: (1) the accuracy in reconstructing the initial signal and (2) the true number of IMFs. These errors can be decreased to a certain degree but need more calculations (Colominas et al., 2014).

IMPROVED CEEMDAN

Improved CEEMDAN is a method to solve the mode mixing problem with the highest accuracy. This method realizes the coherence in frequency between adjoining scales by including a certain percent of white noise which follows the weakening in mode mixing problem and uncertainty in the number of intrinsic mode functions (Colominas et al., 2014; Zhang et al., 2018). Improved CEEMD with adaptive noise, has a simple algorithm based on EMD written below.

In order to demonstrate the eminence of improved CEEMD with adaptive noise, we compare the error of the CEEMDAN and the ICEEMDAN for the signal shown in Fig. 2.

Algorithm 2 Improved CEEMD with adaptive noise

Inputs:

Initial signal as x
White Noise as $w^{(i)}$
Noise level as β_0
Number of noise realization as NR
Maximum iteration as MaxIt

Outputs:

IMFs
Residual

function ICEEMDAN
  $n = 1$ ▷ n = number of IMFs
  SNR enhancement = True
  IMFs = {}
  while amplitude of $x^{(i)} \neq 0$ || number of extermas $x^{(i)} \geq 2$ **do**
    for $i = 1, \cdots,$ NR **do**
      $x^{(i)} = x + \beta_{i-1} E_n(w^{(i)})$ ▷ $E_n(w^{(i)})$ = $IMF_n(w^{(i)})$ derived with EMD
      i = i+1
      EMD(x^i)
      calculate n^{th} IMF of $x^{(i)}$
      return $IMF_n = E_n$
      $Z(x^i) + \beta_{n-1} E_{n+1}(w^{(i)}) = r_i + \beta_{n-1} E_{n+1}(w^{(i)})$ ▷ constructing next signal
      EMD($r_n + \beta_{n-1} E_{n+1}(w^{(i)})$)
      $IMF_n = r_n - \beta_{n-1} E_{n+1}(w^{(i)})$ ▷ calculate next IMF
      return IMF_n
      n = n+1
    end for
    $x^{(i)} = x - IMF_{(1, \cdots, n)}$
  end while
  return IMFs, Residual
end function
Close all processes

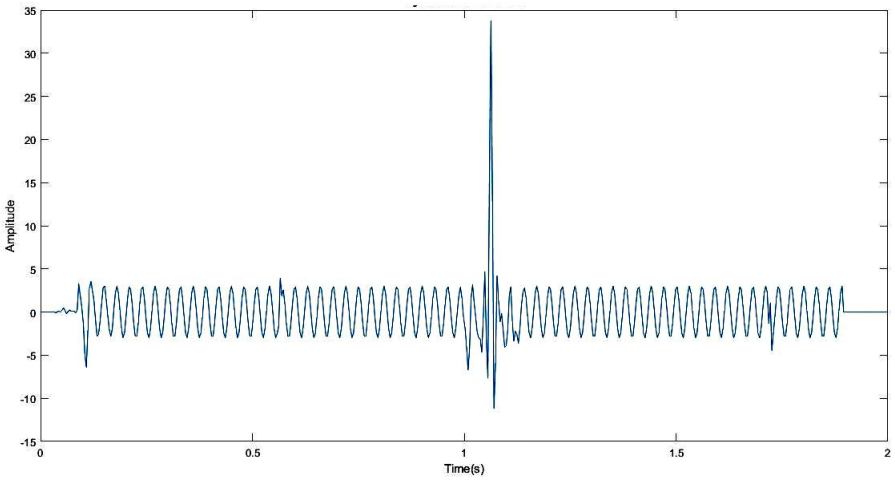

(a)

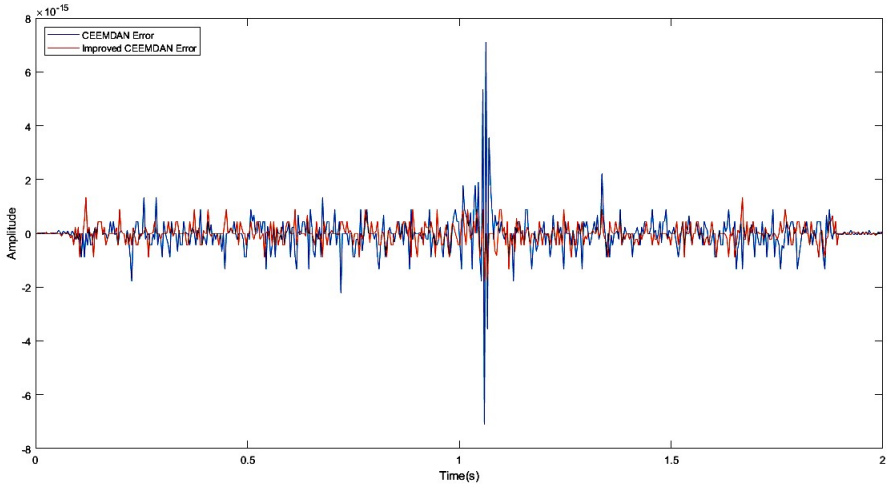

(b)

Fig. 2. Synthetic signal with background 15 Hz Cosine wave (a) ICEEMDAN and CEEMDAN errors for the synthetic signal (b).

PROPOSED METHOD FOR INVERSION

Seismic impedance inversion is a conventional method to obtain quantitative description of subsurface rocks' properties using seismic and well log data (Fu, 2004; Madiba and McMechan, 2003; Pendrel, 2006; Riedel et al., 2009). The purpose of well log data in impedance inversion is that the initial impedance model comes from low frequency P-wave and porosity logs. Well log data is containing frequencies within zero to more

than 200 Hz. There are various suggested workflows for band-limited impedance inversion (Liu et al., 2015; Lloyd, 2013; Maurya and Singh, 2015). The mathematical steps for this method begin with:

$$R_i = \left(\frac{Z_{i+1}-Z_i}{Z_{i+1}-Z_i}\right) \quad . \tag{8}$$

Eq. (8) defines the first step of the workflow to obtain acoustic impedance from seismic trace with impedance estimation where R_i is the reflectivity coefficient series, and Z_i is the acoustic impedance of the i-th subsurface layer.

In order to solve eq. (8) to get a series of impedance for the n-th layer model, eq. (8) can be changed to:

$$\begin{aligned} Z_{i+1} &= Z_i\left(1+\frac{2R_i}{1-Ri}\right) \\ &= Z_i\left(\frac{1+R_i}{1-R_i}\right). \end{aligned} \tag{9}$$

Eq. (9) calculates acoustic impedance for the next layer

$$\begin{aligned} &Z \\ &= Z_1\left(\frac{1+R_1}{1-R_1}\right)\left(\frac{1+R_2}{1-R_2}\right)\ldots\left(\frac{1+R_{n-1}}{1-R_{n-1}}\right) \quad . \end{aligned} \tag{10}$$

In the next step, acoustic impedance for the n-th layer can be calculated through eq. (10)

$$Z_{i+1} = Z_i \prod_{k=1}^{i}\left(\frac{1+R_k}{1-R_k}\right). \tag{11}$$

Eq. (11) is another representation of eq. (10). The presented solution in eq. (11) is dependent on knowing the first layer's impedance in the model. Suppose eq. (11) is divided by the first layer's impedance, and a natural logarithm had been taken of it. In that case, the relationship between seismic trace and acoustic impedance can be obtained through eq. (12)

$$\ln\left(\frac{Z_{i+1}}{Z_1}\right) = \sum_{k=1}^{i} \ln\left(\frac{1+R_k}{1-R_k}\right)$$

$$\approx 2\sum_{k=1}^{i} R_k. \tag{12}$$

$$Z_{i+1} = I_1 \exp\left(2\sum_{k=1}^{i} R_k\right). \tag{13}$$

In the last step, an approximation for the natural logarithm term in eq.(12) is needed which is valid for small *R*. By solving eq. (12) for Z_{i+1}, eq.(13) results.

$$Z_{i+1} = I_1 \exp\left(\gamma\sum_{k=1}^{i} S_k\right). \tag{14}$$

To make the seismic trace as a scaled reflectivity model, eq. (14) is resulting regarding $S_k = \frac{2R_k}{\gamma}$ which depends on γ that it is a scaling factor defined by numerical estimates.

Eq. (14) is the body of the band-limited inversion, which combines the seismic traces and exponentiates the result to calculate an impedance trace same as the prior proposed calculation (Maurya et al., 2020; Schuster, 2017) but with a few modifications in the *preconditioning* phase. A considerable restriction of the Band-limited inversion is that the seismic data must be in zero phase; otherwise, it can be transformed to it with known methods. Due to the nature of oil and gas and reservoir rocks' properties, usually potential hydrocarbon reservoirs can be found in low impedance zones (Maurya et al., 2020; Schuster, 2017; Wang, 2016).

According to Fig. 3, the proposed method uses the residual mode function as the linear trend that contains the lowest frequencies in the initial signal (Jicheng et al., 2020; Xue et al., 2019; Zhang et al., 2018). However, the previous methods are using the least-squares approach to fit a line to the impedance log (Maurya et al., 2020).

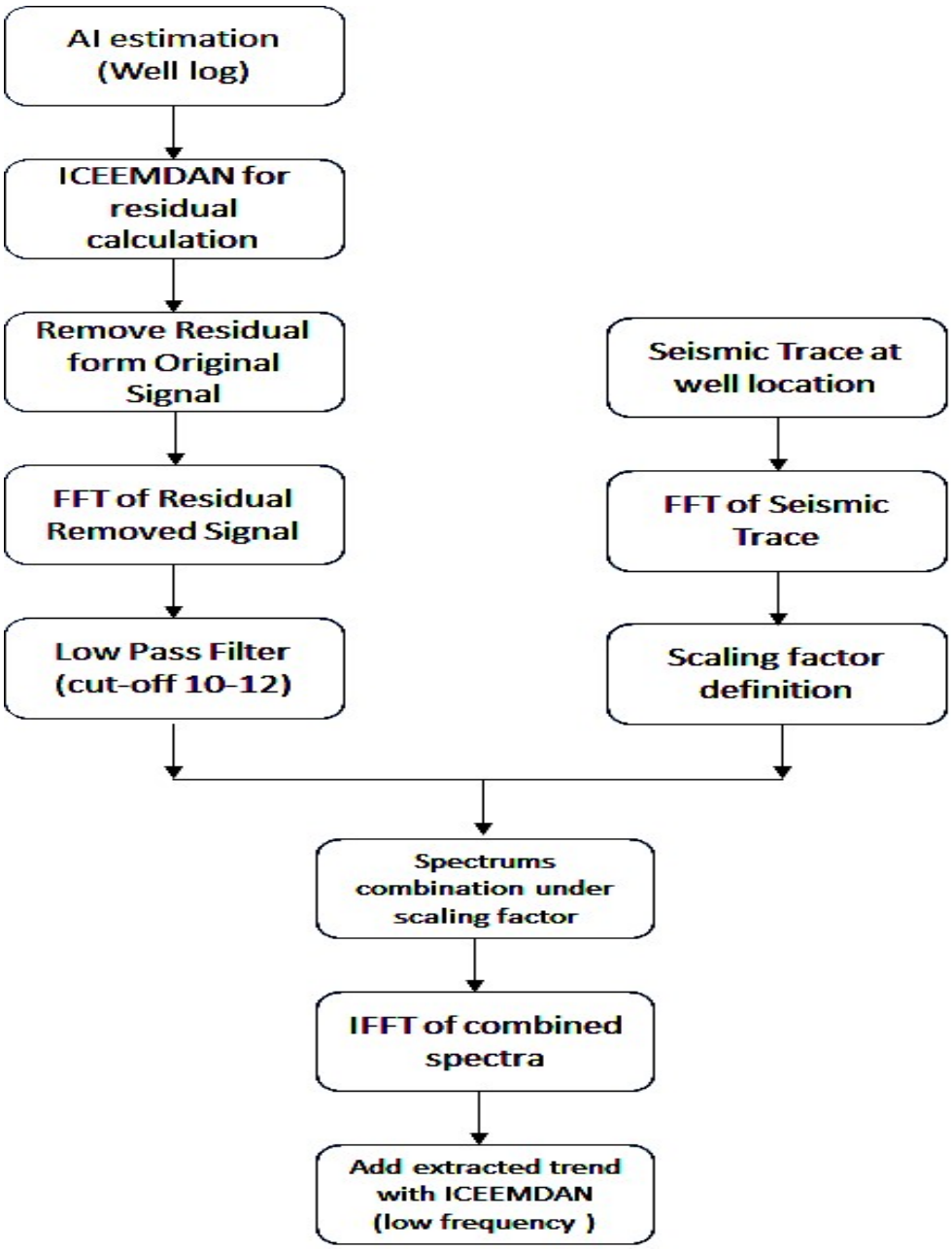

Fig. 3. Workflow for the proposed impedance inversion method.

The linear trend estimated by the ICEEMDAN has merit in comparison to the least-squares linear regression method, and will result in a more precise linear trend. The residual function won't contain any mid to high-frequency components, and it will provide a more robust approximation for the log's impedance linear trend.

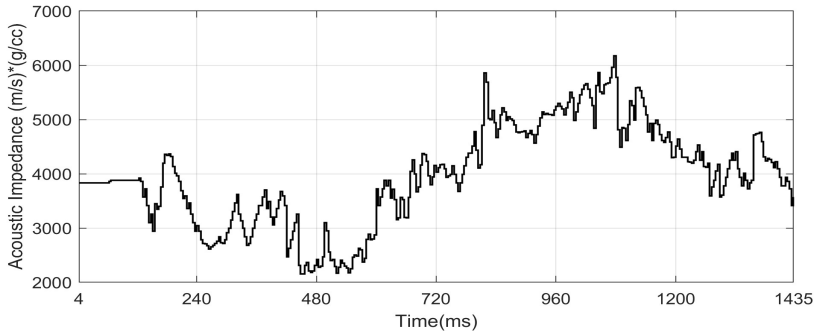

(a)

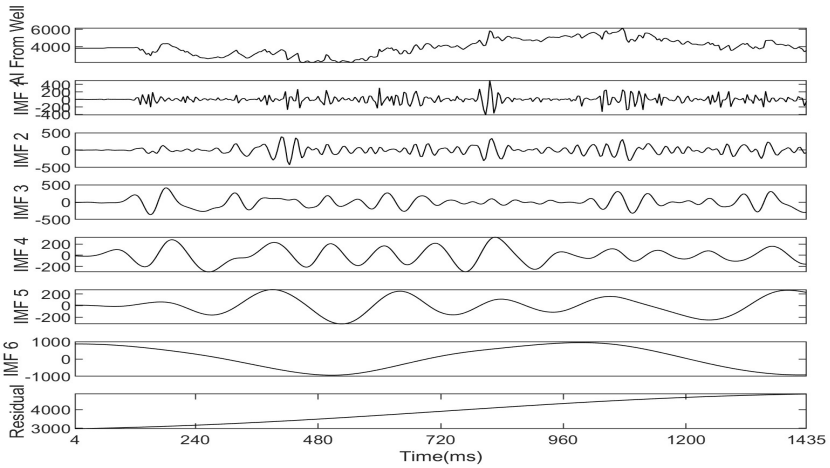

(b)

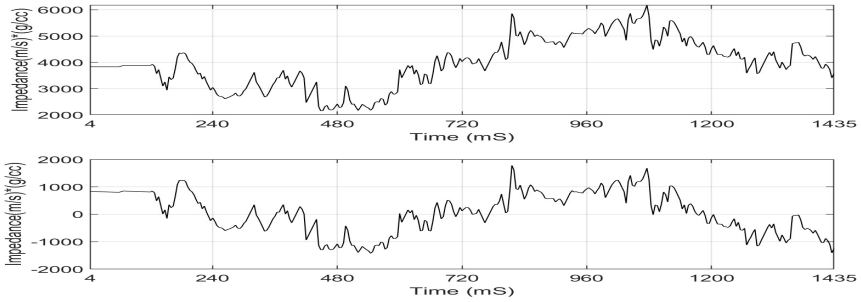

(c)

Fig. 4. Step-by-step *Preconditioning* phase for inversion: Well impedance (a), ICEEMDAN (b) on AI, Removing linear trend (c).

RESULTS and DISCUSSION

In this section, we compare the inverted impedance by the represented method in this research with hard and soft constrained Model-based as well as the Band-limited seismic inversion methods for real seismic data.

For impedance inversion, we used the well F02-01 and seismic inline 362 from open access F3 Netherlands Block V6 dataset published in 2016. According to the suggested workflow, the outcomes of the proposed impedance inversion method steps are shown in Fig. 4, which illustrates the *Preconditioning* phase for target well.

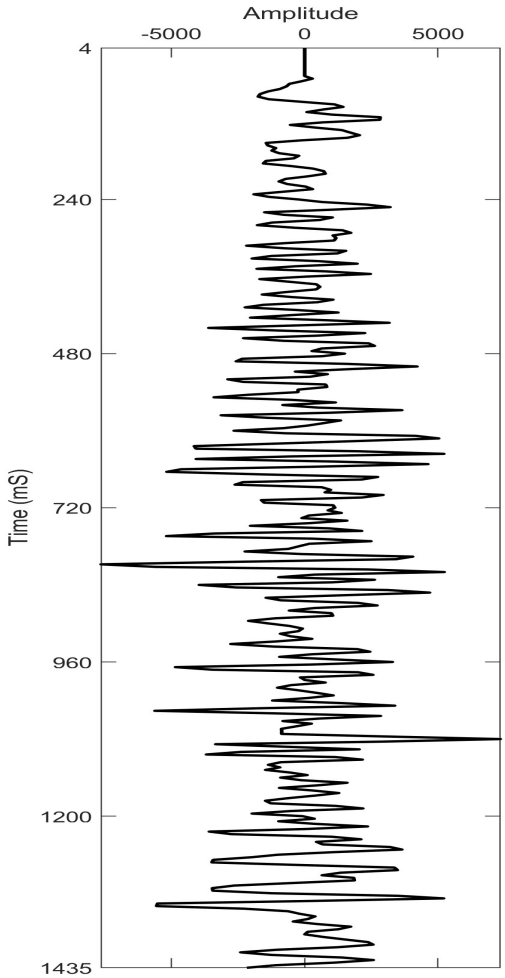

Fig. 5. Seismic trace at well location.

Fig. 6 shows the results of the proposed approach and other commercial inversion methods for calculating acoustic impedance from the seismic trace at well location is shown in Fig. 5 with more accurate low-frequency data derived from impedance log by using the improved CEEMD with adaptive noise method.

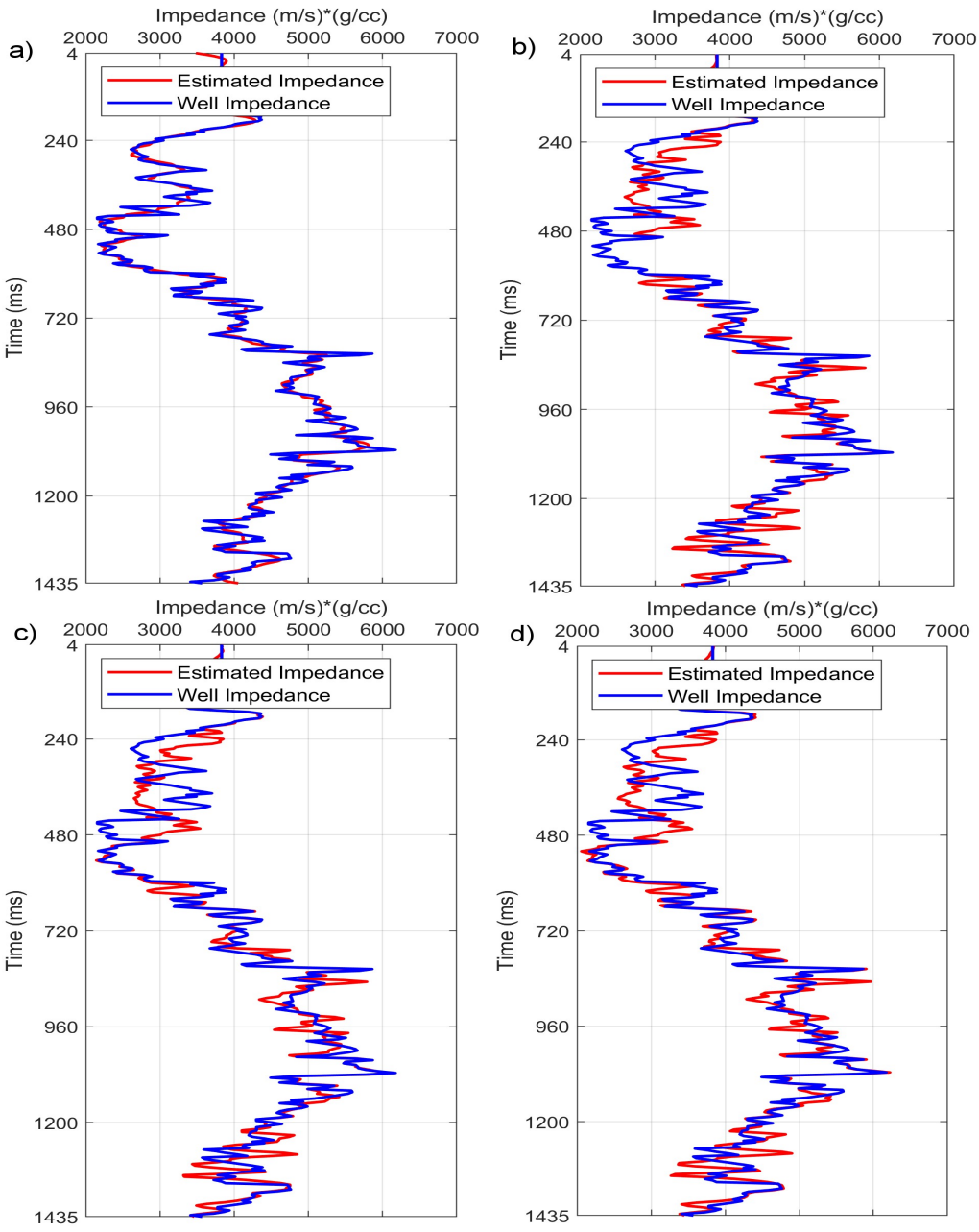

Fig. 6. Acoustic Impedance calculated by proposed approach (a), band-limited inversion (b), hard constrained model-based (c), and soft constrained model-based (d) inversion methods at well location in comparison with the impedance log.

In order to ascertain the eminence and validate the proposed method in this study, the inverted log derived from the proposed method and the Band-limited impedance as well as both hard and soft constrained Model-based inversion methods have been compared with the original impedance log in Fig. 6. The correlation coefficient for the proposed algorithm is 98.44%, and the RMS error is 164.82.

By and large, the examination of Fig. 7, which shows the cross plots between the original and inverted impedance logs and Table 1 verifies that the proposed algorithm has improved the acoustic impedance estimation, and it has a considerable accuracy in comparison to other common methods. This method is also insensitive to the overall scale of the seismic data like previous methods.

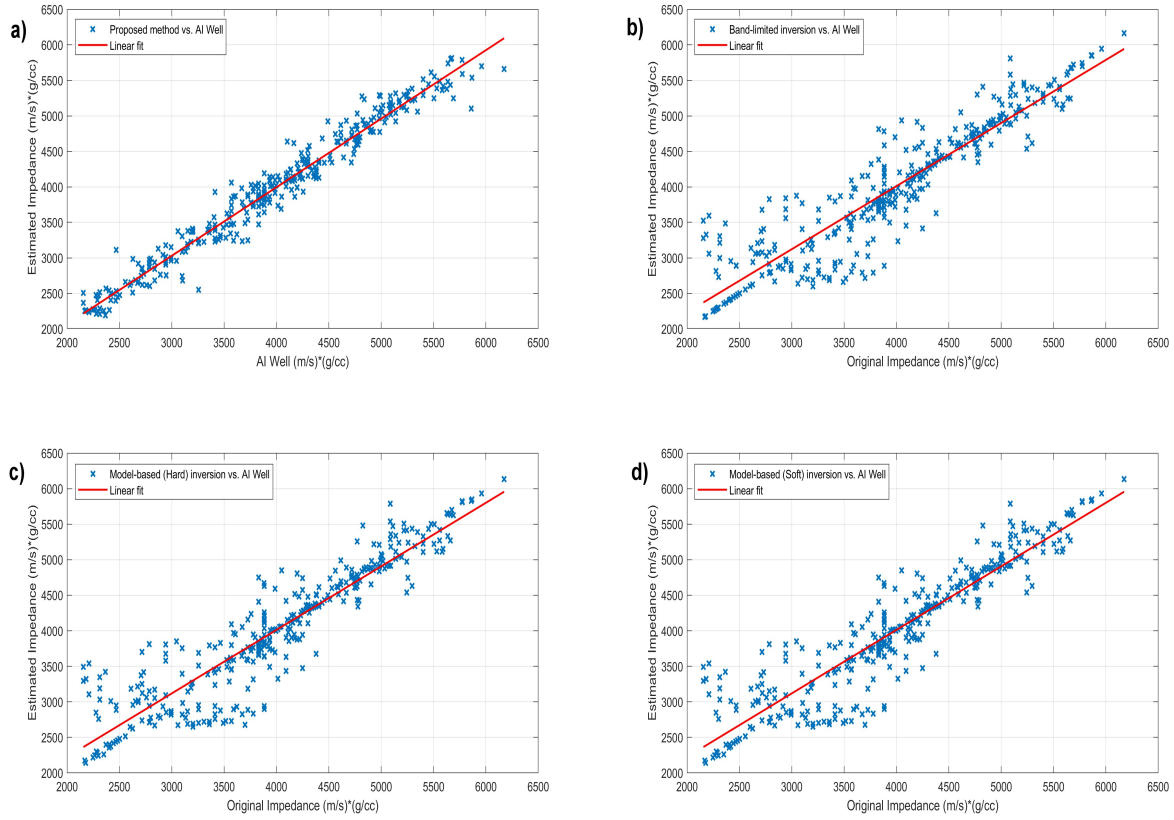

Fig. 7. Cross plots between original and inverted impedance for proposed method (a), bandlimited inversion (b), hard constrained model-based (c), and soft constrained model-based (d) inversion methods.

Table 1. Comparison of the proposed method with common methods for Well F02-01.

Method	Correlation Coefficient(%)	RMS Error
Band-limited inversion	91.29	345.33
Model-based inversion (Hard)	91.12	322.39
Model-based inversion (Soft)	93.05	295.48
Proposed method	98.44	164.82

For the seismic section (inline 362) shown in Fig. 8, which has complex geological features, acoustic impedance was calculated by the proposed method as well as other common inversion methods used in geophysical reservoir characterization.

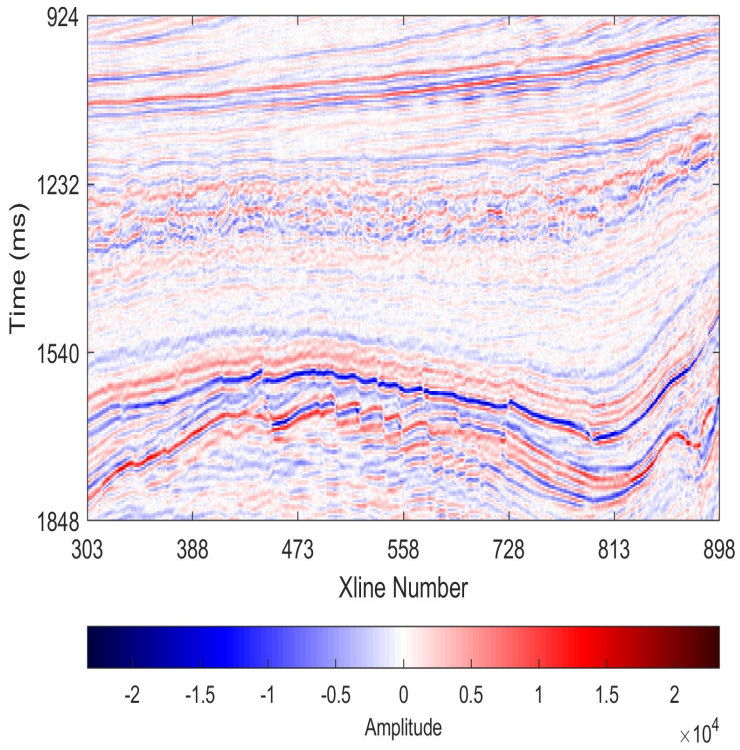

Fig. 8. Seismic section (inline 362), blue color illustrates low amplitude and red shows high amplitude values.

Fig. 9 shows the inversion results for the seismic section shown in Fig. 8 using the Band-limited, hard, and soft constrained Model-based inversion methods, respectively. The proposed method has better resolution than the other methods. Simultaneously, the low impedance layers in inline 362 are potential hydrocarbon existent zones and the black arrows in Fig. 9 are showing the potential reservoir units in this seismic inline.

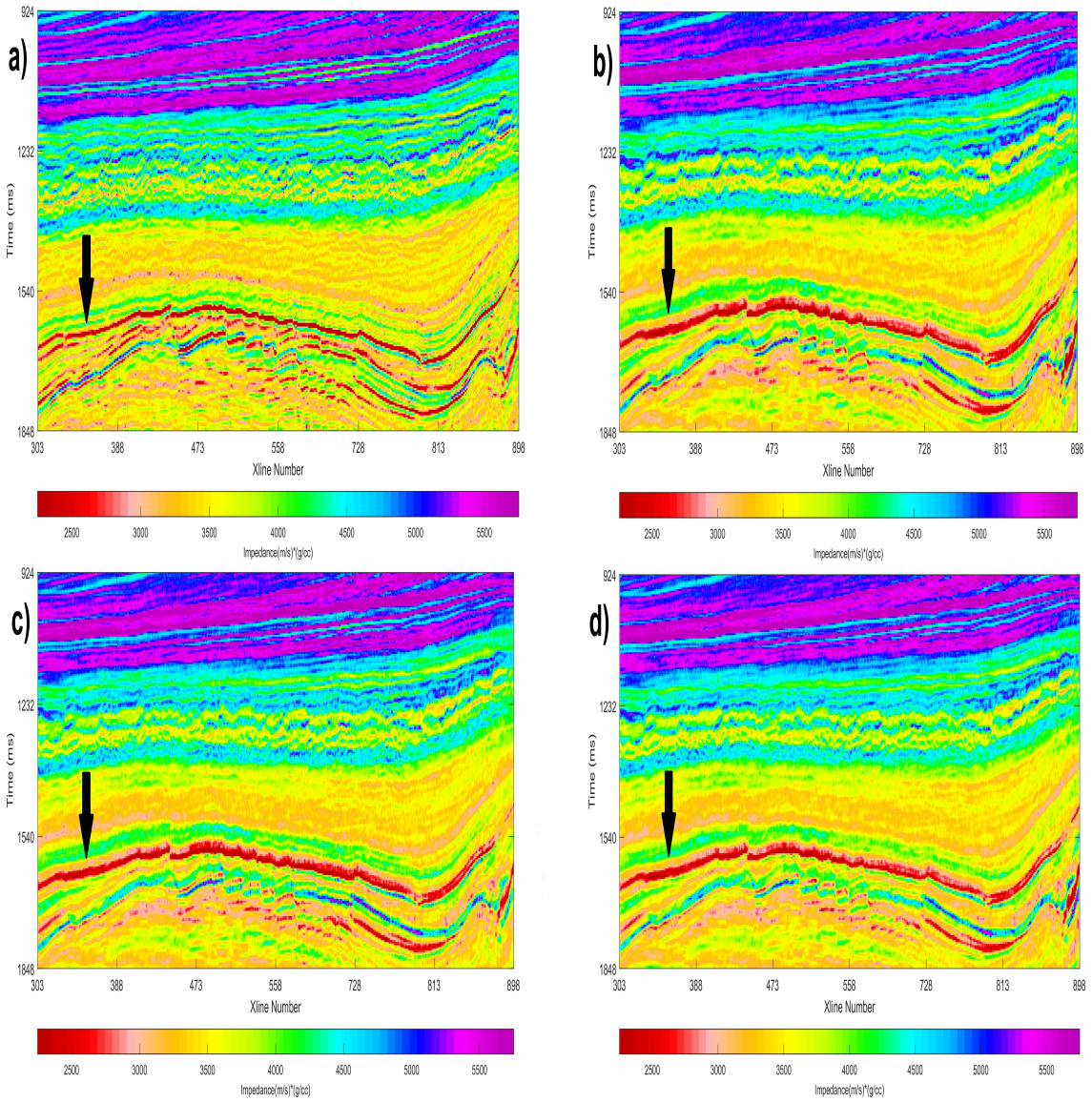

Fig. 9. Inverted seismic sections by proposed method (a), band-limited (b), hard constrained model-based (c), and soft constrained model-based (d) inversion methods for the seismic image shown in Fig. 8, red and purple colors illustrating low and high impedance values.

The correlation coefficients and RMS errors are shown in Table 2 for other available wells in the data.

Table 2. Results of the proposed method for other available wells in data.

Well	Correlation Coefficient(%)	RMS Error
F 03-02	98.78	305.24
F 03-04	95.63	132.16
F 06-01	97.74	173.65

In order to obtain the best impedance image from the seismic section shown in Fig. 8, through numerous experiments, we used the presented parameters in Table 3 in our proposed algorithm. Based on our numerical experiments, we suggest to set the number of noise realization parameter between 100 and 1000 which affects the accuracy in calculating the IMFs.

Table 3. Parameters for signal decomposition.

Parameter	Value
Noise standard deviation	0.2
Number of noise realizations	150
Maximum iteration	100

Since improved CEEMD with adaptive noise is a fully data-driven signal decomposition method, selecting the best values for inversion parameters in our proposed method is a critical job. The quality of seismic data and well logging are essential factors. The dominant lithology in the target area is also an important property in any seismic inversion algorithm. Since the processing time is another factor in our proposed algorithm, based

on our numerical experiments, increasing the number of noise realization and maximum iteration parameters adversely affects the processing time for seismic data, leading us to a time-consuming operation.

CONCLUSION

We combined the improved CEEMDAN and the band-limited impedance inversion algorithm to acquire more accurate subsurface layer-based information. This gives more precise information which is required to obtain accurate petrophysical parameters for any geophysical studies in reservoir characterization. In other words, our Impedance inversion method has demonstrated an improved inversion procedure in comparison to the previous methods by an implementation of a spectral decomposition method called ICEEMDAN in seismic post-stack inversion procedure. The proposed method amends the common approaches to analyze the frequency content of the impedance log or estimation by extracting the trend of it with higher accuracy. Unlike the previous ones, this method does not use the least-squares linear regression and leads us to engender subsurface images with higher resolution by producing a more robust low-frequency model. It has an impressive advantage over other commercial post-stack inversion methods used in seismic exploration, interpretation, and reservoir characterization. These mentioned tools have a significant role in geophysics, petroleum, and geothermal industries.

The most crucial circumstance about our work is that the proposed algorithm depends on a few additional parameters compared to the other common post-stack inversion methods. This is due to the ICEEMDAN signal decomposition tool. These parameters are; (1) the number of noise realizations, (2) the value of noise in the deviation procedure which authors suggest that 0.20 would be appropriate, and (3) the maximum number of iterations. Each of these parameters can influence the final result, consequently, the resolution of the subsurface impedance images. To facilitate this post-stack inversion method, the authors suggest testing and classifying the mentioned parameters for various lithologies in any area to acquire the subsurface impedance images with the highest resolution possible. For Well F 02-01 in the F3 block Netherlands V6 dataset published in 2016, our method resulted in a 98.44(%) correlation coefficient with 164.82 RMS error between the original log and inverted log while the commercial Band-limited, hard and soft constrained Model-based inversion methods resulted 91.29(%) and 91.12(%) and 93.05(%) with 345.33, 322.39 and 295.48 RMS errors respectively.

REFERENCES

Alvarez, P., Bolıvar, F., Di Luca, M., and Salinas, T., 2015. Multiattribute rotation scheme: A tool for reservoir property prediction from seismic inversion attributes. Interpretation, 3(4): SAE9–SAE18.

Amundsen, L. and Landrø, M., 2013. Broadband seismic technology and beyond: Part I: The drive for better bandwidth and resolution. GeoExplor., 10: 78-82.

Bekara, M. and van der Baan, M., 2009. Random and coherent noise attenuation by empirical mode decomposition. Geophysics, 74(5): V89-V98.

Carrazzone, J.J., Chang, D., Lewis, C., Shah, P.M. and Wang, D.Y., 1996. Method for deriving reservoir lithology and fluid content from pre-stack inversion of seismic data. Google Patents. (US Patent 5,583,825)

Chen, Q. and Sidney, S., 1997. Seismic attribute technology for reservoir forecasting and monitoring. The Leading Edge, 16: 445-448.

Colominas, M.A., Schlotthauer, G. and Torres, M.E., 2014. Improved complete ensemble EMD: A suitable tool for biomedical signal processing. Biomedic. Sign. Process. Contr., 14: 19-29.

Das, V., Pollack, A., Wollner, U. and Mukerji, T., 2018. Convolutional neural network for seismic impedance inversion. Expanded Abstr., 88th Ann. Internat. SEG Mtg., Anaheim: 2071-2075.

Ferguson, R.J. and Margrave, G.F., 1996. A simple algorithm for band-limited impedance inversion. CREWES Research Report, 8(21), 1-10.

Flandrin, P., Rilling, G. and Goncalves, P., 2004. Empirical mode decomposition as a filter bank. IEEE Sign. Process. Lett., 11: 112-114.

Fnegqi, Q., Ya, W., Menghua, W., Xiaoying, F., Fusong, X., Haoqiang, L. and Jing, J., 2014. Application of pre-stack and post-stack seismic multi-attribute inversion for oil and gas inspection of Niudong Buried Hill. China Petrol. Explor., 19(2), 39-45.

Fu, L.-Y., 2004. Joint inversion of seismic data for acoustic impedance. Geophysics, 69: 994-1004.

Gholami, A., 2016. A fast automatic multichannel blind seismic inversion for highresolution impedance recovery. Geophysics, 81(5): V357-V364.

Grant, S.R., Hughes, M.J., Smith, S.R., Gasimov, A. and Pickard, M.C., 2017. One-dimensional stochastic inversion for seismic reservoir characterization - a case study. The Leading Edge, 36: 886–894.

Han, J. and van der Baan, M., 2011. Empirical mode decomposition and robust seismic attribute analysis. Abstr., CSPG CSEG CWLS Conv., Vol. 114.

Han, J. and van der Baan, M., 2013. Empirical mode decomposition for seismic time-frequency analysis. Geophysics, 78(2): O9-O19.

Haris, A., Novriyani, M., Suparno, S., Hidayat, R. and Riyanto, A., 2017. Integrated seismic stochastic inversion and multi-attributes to delineate reservoir distribution, Case study MZ fields, Central Sumatra basin. AIP Conf. Proc. , Vol. 1862: 030180.

Huang, N. E., Shen, Z., Long, S. R., Wu, M. C., Shih, H. H., Zheng, Q., ... Liu, H. H. (1998). The empirical mode decomposition and the hilbert spectrum for nonlinear and non-stationary time series analysis. Proceedings of the Royal Society of London. Series A: mathematical, physical and engineering sciences, 454(1971), 903–995.

Huang, N.E. and Wu, Z., 2008. A review on Hilbert-Huang transform: Method and its applications to geophysical studies. Rev. Geophys., 46(2).

Jicheng, L., Gu, Y., Chou, Y. and Gu, J., 2020.. Seismic data random noise reduction using a method based on improved complementary ensemble EMD and adaptive interval threshold. Explor. Geophys., 52: 137-149.

Kushwaha, P.K., Maurya, S., Singh, N. and Rai, P., 2020. Use of maximum likelihood sparse spike inversion and probabilistic neural network for reservoir characterization: a study from F-3 block, The Netherlands. J. Petrol. Explor. Product. Technol., 10: 829-845.

Latimer, R.B., Davidson, R. and van Riel, A., 2000. An interpreter's guide to understanding and working with seismic-derived acoustic impedance data. The Leading Edge, 19: 242-256.
Li, K., Yin, X., Liu, J. and Zong, Z.,2019.. An improved stochastic inversion for joint estimation of seismic impedance and lithofacies. J. Geophys. Engineer., 16: 62-76.
Lindseth, R.O., 1979. Synthetic sonic logs - a process for stratigraphic interpretation. Geophysics, 44: 3-26.
Liu, C., Song, C., Lu, Q., Liu, Y., Feng, X. and Gao, Y., 2015. Impedance inversion based on l1- norm regularization. J. Appl. Geophys., 120: 7-13.
Lloyd, H., 2013. An investigation of the role of low frequencies in seismic impedance inversion (Unpublished M.Sc. thesis). Graduate Studies, Univ. of Calgary, Calgary.
Madiba, G.B. and McMechan, G.A., 2003. Seismic impedance inversion and interpretation of a gas carbonate reservoir in the Alberta Foothills, Western Canada. Geophysics, 68: 1460-1469.
Maurya, S. and Singh, K., 2015. Estimation of seismic parameters from prestack inversion. Abstr., 2nd Internat. Conf. Comp. Exp. Sci. Engineer. (ICCESEN), Antalya, Turkey.
Maurya, S.P. and Singh, N.P., 2019. Estimating reservoir zone from seismic reflection data using maximum-likelihood sparse spike inversion technique: a case study from the Blackfoot Field (Alberta, Canada). J. Petrol. Explor. Product. Technol., 9: 1907-1918.
Maurya, S.S., Singh, N. and Singh, K., 2020. Seismic Inversion Methods: A Practical Approach. Springer Verlag, Berlin.
Mhamdi, F., Poggi, J. and Jaidane, M., 2010. Empirical mode decomposition for trend extraction: application to electrical data. Abstr., 19th Internat. Conf. Computat. Statist., Paris.
Pendrel, J., 2006. Seismic inversion - a critical tool in reservoir characterization. Scandinav. Oil-Gas Magaz., 5(6): 19-22.
Ray, A.K. and Chopra, S., 2016. Building more robust low-frequency models for seismic impedance inversion. First Break, 34(5), 29-34.
Riedel, M., Bellefleur, G., Mair, S., Brent, T.A. and Dallimore, S.R., 2009. Acoustic impedance inversion and seismic reflection continuity analysis for delineating gas hydrate resources near the Mallik research sites, Mackenzie Delta, Northwest Territories, Canada. Geophysics, 74(5): B125-B137.
Russell, B.H., 1988. Introduction to Seismic Inversion Methods. SEG, Tulsa, OK.
Schuster, G.T., 2017. Seismic Inversion. SEG, Tulsa, OK.
Shang, Z., Yuan, L. and Gong, Y., 2015. EMD interval thresholding denoising based on correlation coefficient to select relevant modes. 34th Chin. Control Conf.: 4801-4806.
Torres, M.E., Colominas, M.A., Schlotthauer, G. and Flandrin, P., 2011. A complete ensemble empirical mode decomposition with adaptive noise. Abstr., IEEE Internat. Conf. Acoust., Speech Sign. Process. (ICASSP), Prague: 4144-4147.
Wang, Y., 2016. Seismic Inversion: Theory and Applications. John Wiley & Sons, New York.
Wu, Z. and Huang, N.E., 2009. Ensemble empirical mode decomposition: a noise-assisted data analysis method. Advan. Adapt. Data Analys., 1: 1–41.
Xue, Y.-J., Cao, J.-X., Du, H.-K., Zhang, G.-L. and Yao, Y., 2016. Does mode mixing matter in EMD-based highlight volume methods for hydrocarbon detection? Experimental evidence. J. Appl. Geophys., 132-210.
Xue, Y.-X., Cao, J.-X., Wang, X.-J., Li, Y.-X. and Du, J., 2019. Recent developments in local wave decomposition methods for understanding seismic data: Application to seismic interpretation. Surv. Geophys., 40: 1185-1210.
Yang, F. and Ma, J., 2019. Deep-learning inversion: A next-generation seismic velocity model building method. Geophysics, 84(4): R583-R599.
Yeh, J.-R., Shieh, J.-S. and Huang, N.E., 2010. Complementary ensemble empirical mode decomposition: A novel noise enhanced data analysis method. Advan. Adapt. Data Analys., 2: 135-156.

Zahmatkesh, I., Kadkhodaie, A., Soleimani, B., Golalzadeh, A. and Azarpour, M., 2018. Estimating VSAND and reservoir properties from seismic attributes and acoustic impedance inversion: A case study from the Mansuri oilfield, SW Iran. J. Petrol. Sci. Engineer., 161: 259-274.

Zhang, J., Guo, Y., Shen, Y., Zhao, D. and Li, M., 2018. Improved CEEMDAN–wavelet transform de-noising method and its application in well logging noise reduction. J. Geophys. Engineer., 15: 775-787.

Zhang, R., Sen, M.K., Phan, S. and Srinivasan, S., 2012. Stochastic and deterministic seismic inversion methods for thin-bed resolution. J. Geophys. Engineer., 9: 611-618.

Zhang, S. and Li, Y., 2020. Seismic exploration desert noise suppression based on complete ensemble empirical mode decomposition with adaptive noise. J. Appl. Geophys., 180: 104055.

Zhou, D., Yin, X. and Zong, Z., 2019. Multi-trace basis-pursuit seismic inversion for resolution enhancement. Geophys. Prosp., 67: 519-531.